

Molecular Outflows in Low- and High-Mass Star Forming Regions

Héctor G. Arce

American Museum of Natural History

Debra Shepherd

National Radio Astronomy Observatory

Frédéric Gueth

Institut de Radioastronomie Millimétrique, Grenoble

Chin-Fei Lee

Harvard-Smithsonian Center for Astrophysics

Rafael Bachiller

Observatorio Astronómico Nacional

Alexander Rosen

Max-Planck-Institut für Radioastronomie

Henrik Beuther

Max-Planck-Institut für Astronomie

We review the known properties of molecular outflows from low- and high-mass young stars. General trends among outflows are identified, and the most recent studies on the morphology, kinematics, energetics, and evolution of molecular outflows are discussed, focusing on results from high-resolution millimeter observations. We review the existing four broad classes of outflow models and compare numerical simulations with the observational data. A single class of models cannot explain the range of morphological and kinematic properties that are observed, and we propose a possible solution. The impact of outflows on their cloud is examined, and we review how outflows can disrupt their surrounding environment, through the clearing of gas and the injection of momentum and energy onto the gas at distances from their powering sources from about 0.01 to a few pc. We also discuss the effects of shock-induced chemical processes on the ambient medium, and how these processes may act as a chemical clock to date outflows. Lastly, future outflow research with existing and planned millimeter and submillimeter instruments is presented.

1. INTRODUCTION

As a star forms by gravitational infall, it energetically expels mass in a bipolar jet. There is strong evidence for a physical link between inflow and outflow and that magnetic stresses in the circumstellar disk-protostar system initially launch the outflowing material (see chapters by *Pudritz et al.*; *Ray et al.*; and *Shang et al.*). The ejected matter can accelerate entrained gas to velocities greater than those of the cloud, thereby creating a molecular outflow. Outflows can induce changes in the chemical composition of their host cloud and may even contribute to the decline of the infall process by clearing out dense gas surrounding the protostar.

In addition, molecular outflows can be useful tools for understanding the underlying formation process of stars of all masses, as they provide a record of the mass-loss history of the system.

Protostellar outflows can be observed over a broad range of wavelengths, from the ultraviolet to the radio. In this review we will concentrate on the general characteristics and properties of molecular outflows, the entrainment process, and the chemical and physical impact of outflows on the cloud that are mainly detected through observations of molecular rotational line transitions at millimeter and submillimeter wavelengths. At these wavelengths the observations mainly trace the cloud gas that has been swept-up

by the underlying protostellar wind, and provide a time-integrated view of the protostar’s mass-loss process and its interaction with the surrounding medium.

2. GENERAL OUTFLOW PROPERTIES

Over the last 10 years, millimeter interferometers have allowed the observation of molecular outflows at high angular resolutions (~ 1 to $4''$), while the capability to observe mosaics of several adjacent fields has enabled mapping of complete outflows at those resolutions. Such interferometric observations give access to the internal structure of the gas surrounding protostars, and can disentangle the morphology and dynamics of the different elements that are present (i.e., protostellar condensation, infalling and outflowing gas). These high resolution observations have been critical to the discovery of the kinematics and morphology of outflows from massive OB (proto)stars, which are typically more than a kiloparsec away.

General trends have been identified in molecular outflows from both low- and high-mass protostars, even though they display a broad diversity of sizes and shapes. These properties have been identified mostly using single-dish and interferometer observations of the CO lines. Molecular outflows exhibit a mass-velocity relation with a broken power law appearance, $dM(v)/dv \propto v^{-\gamma}$, with the slope, γ , typically ranging from 1 to 3 at low outflow velocities, and a steeper slope at higher velocities — with γ as large as 10 in some cases (e.g., *Rodríguez et al.*, 1982; *Lada and Fich*, 1996; *Ridge and Moore*, 2001). The slope of the mass-velocity relation steepens with age and energy in the flow (*Richer et al.*, 2000). The velocity at which the slope changes is typically between 6 and 12 km s^{-1} although outflows can have CO break velocities as low as about 2 km s^{-1} and, in the youngest CO outflows, it can be high as 30 km s^{-1} (see, e.g., *Richer et al.*, 2000, and references therein). The mass, force, and mechanical luminosity of molecular outflows correlate with bolometric luminosity (*Bally and Lada*, 1983; *Cabrit and Bertout*, 1992; *Wu et al.*, 2004), and many fairly collimated outflows show a linear velocity-distance relation, typically referred to as the “Hubble-law”, where the maximum radial velocity is proportional to position (e.g., *Lada and Fich*, 1996). Also, the degree of collimation of outflows from low- and high-mass systems appears to decrease as the powering source evolves (see below).

These observed general trends are consistent with a common outflow/infall mechanism for forming stars with a wide range of masses, from low-mass protostars up to early B protostars. Although there is evidence that the energetics for at least some early-B stars may differ from their low-mass counterparts, the dynamics are still governed by the presence of linked accretion and outflow. A few young O stars show evidence for accretion as well although this is not as well established as for early-B stars (e.g., *van der Tak and Menten*, 2005; chapter by *Cesaroni et al.*).

2.1 Outflows from low-mass protostars

Since their discovery in the early eighties, molecular outflows driven by young low-mass protostars (i.e. typically $< 1 M_{\odot}$) have been extensively studied, giving rise to a detailed picture of these objects (see, e.g., the reviews by *Richer et al.*, 2000; *Bachiller and Tafalla*, 1999, and references therein). The flows typically extend over 0.1–1 parsec, with outflowing velocities of 10–100 km s^{-1} . Typical momentum rates of $10^{-5} M_{\odot} \text{ km s}^{-1} \text{ yr}^{-1}$ are observed, while the molecular outflow mass flux can be as high as $10^{-6} M_{\odot} \text{ yr}^{-1}$ (*Bontemps et al.*, 1996). Particular interest has been devoted to the outflows driven by the youngest, embedded protostars (age of a few 10^3 to a few 10^4 years, the Class 0 objects). These sources are still in their main accretion phase and are therefore at the origin of very powerful ejections of matter.

2.1.1. Molecular jets. The collimation factor (i.e., length/width, or major/minor radius) of the CO outflows, as derived from single-dish studies, range from ~ 3 to > 20 . There is however a clear trend of higher collimation at higher outflowing velocities (see, e.g., *Bachiller and Tafalla*, 1999). Interferometric maps have revealed even higher collimation factors, and, in some cases, high-velocity structures that are so collimated (opening angles $< a$ few degrees) that they can be described as “molecular jets”.

HH 211 is the best example to date of such a molecular jet (*Gueth and Guilloteau*, 1999). At high-velocity, the CO emission is tracing a highly-collimated linear structure that is emanating from the central protostar. This CO jet terminates at the position of strong H_2 bow-shocks, and shows a Hubble law velocity relation. Low-velocity CO traces a cavity that is very precisely located in the wake of the shocks. These observations strongly suggest that the propagation of one or several shocks in a protostellar jet entrain the ambient molecular gas and produces the low-velocity molecular outflow (see Sec. 3). With an estimated dynamical timescale of $\sim 10^3$ years, HH 211 is obviously an extremely young object. Other examples of such highly-collimated, high-velocity jets include IRAS 04166+2706 (*Tafalla et al.*, 2004) and HH 212 (*Lee et al.*, 2000) – these sources are or will be in the near future the subject of more detailed investigations.

In at least SVS 13B (*Bachiller et al.*, 1998, 2000), and NGC1333 IRAS 2 (*Jørgensen et al.*, 2004), NGC1333 IRAS 4 (*Choi* 2005) and HH 211 (*Chandler and Richer*, 2001; *Hirano et al.*, 2006; *Palau et al.*, 2006) the SiO emission traces the molecular jet and *not* the strong terminal shocks against the interstellar medium. This came as a surprise, as it seems to contradict the widely accepted idea that SiO is a tracer of outflow shocks, where the density is increased by several order of magnitudes (e.g., *Martín-Pintado et al.*, 1992; *Schilke et al.*, 1997; *Gibb et al.*, 2004). The lack of significant SiO emission in the terminal shocks suggests that the formation process of this molecule has a strong dependence on the shock conditions (velocity, den-

sity) and/or outflow age (see Sec. 4.2).

The exact nature of these CO and SiO molecular jets is not yet clear. Three basic scenarios could be invoked, in which the high-velocity CO and SiO molecules (*a*) belong to the actual protostellar jet, (*b*) are entrained along the jet in a turbulent cocoon (e.g., *Stahler, 1994; Raga et al., 1995*), or (*c*) are formed/excited in shocks that are propagating down the jet (“internal working surfaces”, *Raga and Cabrit, 1993*). This latter scenario would reconcile the observation of SiO in the jet and the shock-tracer nature of this molecule. The predictions of these three cases, both in terms of line properties and observed morphologies, are somewhat different but the current observations have not yet provided a clear preference for one of these scenarios.

2.1.2. More complex structures. Not all sources have structures as simple or unperturbed as the molecular jets discussed above. CO observations have also revealed a number of more complex outflow properties.

Episodic ejection events seem to be a common property of young molecular outflows. In sources such as, e.g., L 1157 (*Gueth et al., 1998*) and IRAS 04239+2436 (HH 300, *Arce and Goodman, 2001b*), a limited number (2 to 5) of strong ejection events have taken place, each of them resulting in the propagation of a large shock. Morphologically, the flow is therefore the superposition of several shocked/outflowing gas structures, while position-velocity diagrams show multiple “Hubble wedges” (i.e., a jagged profile; *Arce and Goodman, 2001a*). In most of the sources, if several strong shocks are not present, a main ejection event followed by several smaller, weaker shocked areas are observed (e.g., L1448: *Bachiller et al., 1990*; HH 111: *Cernicharo et al., 1999*; several sources: *Lee et al., 2000, 2002*). As noted before, even the molecular jets could include several internal shocks. Altogether, these properties suggest that the ejection phenomenon in young outflows is intrinsically episodic, or — a somewhat more attractive possibility — could be continuous but include frequent ejection bursts. This could be explained by sudden variations in the accretion rate onto the forming star, that result in variations of the velocity of the ejected matter, hence the creation of a series of shocks.

Precession of the ejection direction has been established in a few sources, like Cep E (*Eisloffel et al., 1996*), and L 1157 (*Gueth et al., 1996, 1998*). In several other objects, the observations reveal bending or misalignment between the structures within the outflows (see e.g., *Lee et al., 2000, 2002*). In fact, when observed at the angular resolution provided by millimeter interferometers, many well-defined, regular bipolar outflows mapped with single-dish telescopes often reveal much more complex and irregular structures, which indicate both temporal and spatial variations of the ejection phenomenon.

Quadrupolar outflows are sources in which four lobes are observed, and seem to be driven by the same protostellar condensation. Several scenarios were proposed to explain these peculiar objects: two independent outflows (e.g., *Anglada et al., 1991; Walker et al., 1993*); one sin-

gle flow with strong limb-brightening, which would thus mimic four lobes (e.g., *Avery et al., 1990*); a single outflow but with a strong precession of the ejection direction (e.g., *Ladd and Hodapp, 1997*). The angular resolution provided by recent interferometric observations have clearly favored the first hypothesis in at least two objects (HH 288, *Gueth et al., 2001*; L 723, *Lee et al., 2002*). In both cases, the two outflows are driven by two independent, nearby protostars, located in the same molecular core. It is however unclear whether the sources are gravitationally bound or not.

2.1.3. Time evolution. There is increasing evidence that outflow collimation and morphology changes with time (e.g., *Lee et al., 2002; Arce and Sargent, in preparation*). The youngest outflows are highly collimated or include a very collimated component, strongly suggesting that jet bow shock-driven models are appropriate to explain these objects. Older sources present much lower collimation factors, or — a somewhat more relevant parameter — wider opening angles, pointing towards wide-angle, wind-driven outflows (see Sec. 3.1.1). In fact, neither the jet-driven nor the wind-driven models can explain the range of morphological and kinematic properties that are observed in all outflows (see Sec. 3.2). This was noted by *Cabrit et al. (1997)*, who compared outflow observations to morphologies and PV diagrams predicted by various hydrodynamical models. More recently, a similar conclusion was obtained by *Lee et al. (2000, 2001, 2002)* from interferometric observations of 10 outflows. One attractive scenario to reconcile all observations is to invoke the superposition of both a jet and a wind component in the underlying protostellar wind and a variation in time of the relative weight between these two components. One possible explanation for this scenario is that at very early ages only the dense collimated part of the wind can break out of the surrounding dense infalling envelope. As the envelope loses mass, through infall and outflow entrainment along the axis (see Sec 4.1), the less dense and wider wind component will break through, entraining the gas unaffected by the collimated component, and will eventually become the main component responsible for the observed molecular outflow.

2.2 Outflows from high-mass protostars

Outflows from more luminous protostars have received increasing attention in recent years with the result that we now have a more consistent understanding of massive outflow properties and their relationship to outflows from lower luminosity objects (see, e.g., recent reviews by *Churchwell, 1999; Shepherd, 2003, 2005; and Cesaroni, 2005*).

Outflows from mid- to early-B type stars have mass outflow rates 10^{-5} to a few $\times 10^{-3} M_{\odot} \text{ yr}^{-1}$, momentum rates 10^{-4} to $10^{-2} M_{\odot} \text{ km s}^{-1} \text{ yr}^{-1}$, and mechanical luminosity of 10^{-1} to $10^2 L_{\odot}$. O stars with bolometric luminosity (L_{bol}) of more than $10^4 L_{\odot}$ generate powerful winds with wind opening angle of about 90° within 50 AU of the star (measured from water masers in and along the flow boundaries and models derived from ionized gas emission ob-

served with resolutions of 20-100 AU, e.g., Orion: *Greenhill et al.*, 1998; MWC 349A: *Tafaya et al.*, 2004). The accompanying molecular flows can have an opening angle of more than 90° (measured from CO outflow boundaries 1000 AU to 0.1 pc from the protostar). The flow momentum rate ($> 10^{-2} M_\odot \text{ km s}^{-1} \text{ yr}^{-1}$) is more than an order of magnitude higher than what can be produced by stellar winds and the mechanical luminosity exceeds $10^2 L_\odot$ (e.g., *Churchwell*, 1999; *Garay and Lizano*, 1999).

Outflows from early-B and late O stars can be well-collimated (collimation factors greater than 5) when the dynamical timescale is less than $\sim 10^4$ years. For a few early B (proto)stars with outflows that have a well-defined jet, the jet appears to have adequate momentum to power the larger scale CO flow, although this relation is not as well established as it is for lower luminosity sources. For example, IRAS 20126+4104 has a momentum rate in the SiO jet of $2 \times 10^{-1} \left(\frac{2 \times 10^{-9}}{\text{SiO}/\text{H}_2} \right) M_\odot \text{ km s}^{-1} \text{ yr}^{-1}$ while the CO momentum rate is $6 \times 10^{-3} M_\odot \text{ km s}^{-1} \text{ yr}^{-1}$ (*Cesaroni et al.*, 1999; *Shepherd et al.*, 2000). Although the calculated momentum rate in the SiO jet is adequate to power the CO flow, the uncertainties in the assumed SiO abundance makes this difficult to prove. Another example is IRAS 18151–1208 in which the H_2 jet appears to have adequate momentum to power the observed CO flow (*Beuther et al.*, 2002a; *Davis et al.*, 2004). A counter example may be the Ceph A HW2 outflow because the momentum rate in the HCO^+ outflow is 20 times larger than that of the observed ionized jet. However, the jet could be largely neutral or there may be an undetected wide-angle wind component (*Gómez et al.*, 1999).

Wu et al. (2004) find that the average collimation factor for outflows from sources with $L_{\text{bol}} > 10^3 L_\odot$ is 2.05 compared with 2.81 for flows from lower luminosity sources. This is true even for sources in which the angular size of the flow is at least five times the resolution. Table 1 of *Beuther and Shepherd* (2005) summarizes our current understanding of massive outflows from low-spatial resolution single-dish studies and gives a summary of and references to 15 massive flows that have been observed at higher spatial resolution using an interferometer. Here, we discuss a few of these sources that illustrate specific characteristics of massive outflows.

2.2.1. Collimated flows. The youngest early-B protostars ($\sim 10^4$ years or less) can be jet-dominated and can have either well-collimated or poorly collimated molecular flows. In a few sources, jets tend to have opening angles, α , between 25° and 30° but they do not re-collimate (e.g., IRAS 20126+4104: *Cesaroni et al.*, 1999; *Moscadelli et al.*, 2005; or IRAS 16547–4247: *Rodríguez et al.*, 2005a). Other sources appear to generate well-collimated jets ($\alpha \sim$ few degrees) that look like scaled up jets from low-luminosity protostars (e.g., IRAS 05358+3543: *Beuther et al.*, 2002b). All these sources are $\lesssim 10^4$ years old — they have not yet reached the main sequence. In at least one case jet activity has continued as long as 10^6 years, although the associated molecular flow has a large opening angle and

complex morphology (HH80–81: *Yamashita et al.*, 1989; *Martí et al.*, 1993).

One possible collimated outflow event may have been traced to a young O5 (proto)star in the G5.89–0.39 UC HII region. The O5 star has a small excess at $3.5 \mu\text{m}$ and is along the axis of two H_2 knots that appear to trace a N-S molecular flow along the direction of the UC HII region expansion (*Puga et al.*, 2005). The N-S molecular flow is unresolved so it is not clear that it is collimated even if the H_2 knots appear to trace a collimated outflow event. Although still circumstantial, the evidence is mounting that the O5 star in G5.89 produced the N-S outflow and thus is forming via accretion (*Shepherd*, 2005, and references therein).

2.2.2. Poorly collimated flows. Poorly collimated molecular flows can be due to: 1) extreme precession of the jet as in IRAS 20126+4124 (*Shepherd et al.*, 2000); 2) a wide-angle wind associated with a jet as in HH 80–81 (*Yamashita et al.*, 1989) or perhaps Ceph A HW2 (e.g., *Gómez et al.*, 1999; *Rodríguez et al.*, 2001); 3) a strong wide-angle wind that has no accompanying jet; or 4) an explosive event as seen in Orion (*McCaughrean and Mac Low*, 1997). In massive flows, collimation factors as high as 4 or 5 in the molecular gas can still be consistent with being produced by wind-blown bubbles if the cloud core is very dense and it is easier for the flow to break out of the cloud rather than widen the flow cavity. Once the flow has escaped the cloud core, the bulk of the momentum is transferred to the interclump medium.

In at least some young early-B stars, both the ionized wind near the central source and the larger scale molecular flow are poorly collimated and there is no evidence for a well-collimated jet. Examples of sources that do not appear to have a collimated jet powering the flow include G192.16–3.82 (*Shepherd and Kurtz*, 1999, and references therein), W75 N VLA 2 (*Torrelles et al.*, 2003, and references therein), AFGL 490 (*Schreyer et al.*, 2006, and references therein) and the SiO flow in G5.89–0.39 (not related to the O5 star discussed above; *Sollins et al.*, 2004; *Puga et al.*, 2005). Sources with poorly collimated flows, no evidence for a jet and a good determination of the dynamical age show that the ages tend to be a few $\times 10^5$ years old and a UC HII region exists around a new ZAMS star.

To date, extremely collimated molecular outflows have not been observed toward sources earlier than B0. It is possible that this is simply a selection effect because O stars form in dense clusters and reach the ZAMS in only a few $\times 10^4$ years. Thus, any collimated outflows may be confused by other flows. In a few cases, outflows appear to be due to a sudden explosive event such as that seen in Spitzer images of shocked gas in G34.26+0.15 (*Churchwell*, personal communication) or the H_2 fingers of Orion. There is now good evidence that Source I in Orion and the Becklin-Neugebauer (BN) object were within a few hundred AU from each other about 500 years ago (*Rodríguez et al.*, 2005b). Such close encounters could disrupt the accretion process and create an explosive outflow as seen in Orion (e.g., *Bonnell et al.*, 2003).

2.2.3. *Evolution.* Early-B stars ($L_{bol} \sim 10^4 L_{\odot}$) generate UC HII regions and reach the ZAMS in $5 - 9 \times 10^4$ years while still accreting and generating strong molecular outflows (e.g., *Churchwell, 1999; Garay and Lizano, 1999*, and references therein). The duration of the accretion phase is about the same as in low-luminosity sources (e.g., $5 - 10 \times 10^5$ years) yet the development of an HII region that expands to encompass the accretion disk midway through the formation process suggests that there is a sharp transition in the physical conditions at the base of the flow where material is lifted off the surface of the disk and collimated.

Well-collimated molecular flows from massive protostars tend to be in systems with ages less than a few times 10^4 years old where the central object has not yet reached the main sequence (e.g., IRAS 05358+3543 is well-collimated over approximately 1 pc). In these young sources the effects of increased irradiation on the disk and disk-wind due to the stellar radiation field are minimal. Poorly collimated flows (opening angle greater than 50° that show no evidence for a more collimated component) are associated with more evolved sources that have detectable UC HII regions and the central star has reached the main sequence.

To account for the differences seen in flow morphologies from early B to late O stars *Beuther and Shepherd (2005)* proposed two possible evolutionary sequences which could result in similar observable outflow signatures. In Fig. 1 we show a schematic of the proposed sequences and explain how the observed outflow morphologies can be related to O and B star evolution.

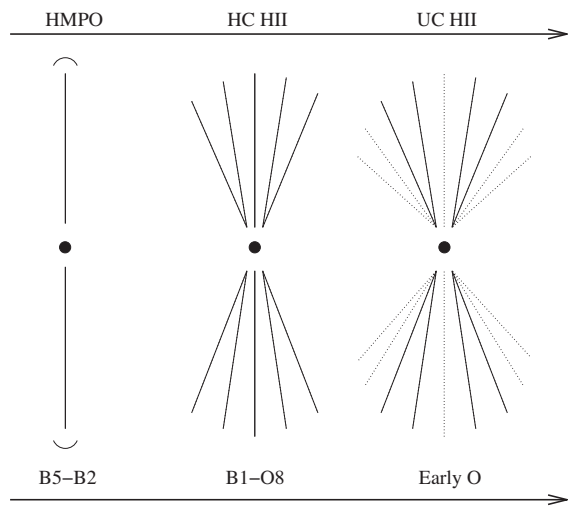


Fig. 1.— Sketch of the proposed evolutionary outflow scenario put forth by *Beuther and Shepherd (2005)*. The three outflow morphologies can be caused by two evolutionary sequences: (top) the evolution of a typical B1-type star from a high-mass protostellar object (HMPO) via a hypercompact HII (HC HII) region to an ultra-compact HII (UC HII) region, and (bottom) the evolution of an O5-type star which goes through B1- and O8-type stages (only approximate labels) before reaching its final mass and stellar luminosity. This evolutionary sequence appears to qualitatively fit the observations, yet it must be tested against both theory and observations.

Once a massive OB star reaches the main sequence, the increased radiation from the central star generates significant Lyman continuum photons and will likely ionize the outflowing gas even at large radii. Inherently lower collimation of the ionized wind due to increased radiation pressure is suggested by the hydrodynamic simulations of *Yorke and Sonnhalter (2002)*. However the radiation pressure is still too low by a factor of 10 to 100 to produce significant changes in the collimation of the observed molecular flows (*Richer et al., 2000*).

The larger photon flux will also increase the ionization degree in the molecular gas and produce shorter ion-neutral collisional timescales. Thus, in principle, this could improve the matter-field coupling, even aiding MHD collimation. However, other effects are likely to counteract this. In particular, if the plasma pressure exceeds the magnetic field pressure and ions are well-coupled to the field, then the outflowing, ionized gas may be able to drag the magnetic field lines into a less collimated configuration (see, e.g., *Königl, 1999; Shepherd et al., 2003*).

Turbulence could also contribute to the decollimation of molecular outflows from massive OB protostars. Increased turbulence in the disk and outflow is expected to weaken the conditions for ideal MHD and hence weaken the collimation effect. Turbulence could be due to higher accretion disk to stellar mass ratios ($M_{disk} > 0.3M_{\star}$) making disks susceptible to local gravitational instabilities, increased radiation pressure and high plasma temperatures. If the ions and neutrals are not well coupled in a turbulent flow then ideal MHD begins to break down and magnetic diffusivity could significantly decollimate the molecular outflow (see, e.g., *Fendt and Cemeljic, 2002*). Further, simulations by *Fendt and Cemeljic* find that the toroidal magnetic field component, B_{ϕ} , decreases with increased turbulence. Since B_{ϕ} is the collimating magnetic component (e.g., *Pudritz & Banerjee, 2005*), such a decrease in B_{ϕ} may contribute to the lower observed collimation for more evolved massive molecular outflows.

3. MOLECULAR OUTFLOW MODELS

3.1 General Overview of Models

Several outflow models have been proposed to explain how molecular outflows from protostars are formed. Currently, outflow models can be separated into four broad classes (*Cabrit et al., 1997*): (1) wind-driven shells, (2) jet-driven bow shocks, (3) jet-driven turbulent flows, and (4) circulation flows. In the first three, molecular outflows represent ambient material that has been entrained by a wide-angle wind or accelerated by a highly collimated jet. In the last class of models, molecular outflows are produced by deflected infalling gas. Most of the work has concentrated on simulating outflows specifically from low-mass protostars, and little work has been done on modeling outflows from high-mass stars. Many flow properties, in particular the CO spatial and velocity structure, are broadly simi-

lar across the entire luminosity range (*Richer et al.*, 2000), suggesting that similar mechanisms may be responsible for the production of molecular outflows from both low- and high-mass systems. Recent results from simulation work on the disk/outflow connection (*Pudritz and Banarjee*, 2005) as well as from observations (*Zhang et al.*, 2002; *Beuther et al.*, 2004) further indicate that molecular outflows from massive stars may be approximately modeled as scaled-up versions of their lower mass brethren.

In the past, most studies used analytical models to try to explain the outflow morphology and kinematics. However, in the last decade computational power has increased sufficiently to allow for multidimensional hydrodynamical (HD) simulations of protostellar outflows that include a simple molecular chemical network. Numerical modeling of the molecular cooling and chemistry, as well as the hydrodynamics, is required in these systems, which are described by a set of hyperbolic differential equations with solutions that are usually mathematically chaotic and cannot be treated analytically. Treatment of the molecular cooling and chemistry facilitates a comparison of the underlying flow with observational quantities (for example, the velocity distribution of mass vs. CO intensity, the temperature distribution of the outflowing gas, and the H₂ 1-0 S(1) maps).

3.1.1. Wind-driven shell models. In the wind-driven shell model, a wide-angle radial wind blows into the stratified surrounding ambient material, forming a thin swept-up shell that can be identified as the outflow shell (*Shu et al.*, 1991; *Li and Shu*, 1996; *Matzner and McKee*, 1999). In these models, the ambient material is often assumed to be toroidal with density $\rho_a = \rho_{ao} \sin^2 \theta / r^2$, while the wind is intrinsically stratified with density $\rho_w = \rho_{wo} / (r^2 \sin^2 \theta)$, where ρ_{ao} is the ambient density at the equator and ρ_{wo} is the wind density at the pole (*Lee et al.*, 2001). This class of models is attractive as it particularly explains old outflows of large lateral extents and low collimation.

In recent years, there have been a few efforts to model wide angle winds numerically. *Lee et al.* (2001) performed numerical HD simulations of an atomic axisymmetric wind and compared it to simulations of bow shock-driven outflows. Their wide-wind models yielded smaller values of γ (see Sec. 2) over a narrower range (1.3–1.8), as compared to the jet models (1.5–3.5). *Raga et al.* (2004b) have included both wide angle winds and bow shock models in a study aimed at reproducing features of the southwest lobe of HH 46/47, with the result that a jet model is able to match enough features that they feel that it is not necessary to invoke a wide angle wind (although it produces a reasonable fit to the observations). In simulations by *Delamarter et al.* (2000) the wind is assumed to be spherical, even though the physical origin of such a wind is not yet clear, and it is focused towards the polar axis by the density gradients in the surrounding (infalling) torus-like environment. In these models the low-velocity γ ranges from approximately 1.3 to 1.5, similar to other studies. The MHD simulations performed by *Gardiner et al.* (2003) show that winds that have a wide opening angle at the base can produce a dense jet-

like structure downstream due to MHD collimation. Very recently, axisymmetric winds have been modeled with a code that includes molecular chemistry and cooling as well as Adaptive Mesh Refinement (AMR) (*Cunningham et al.*, 2005). These last two studies produce satisfactory general outflow lobe appearance, however, no mass-velocity, position-velocity maps, or channel maps have been generated to compare with observations.

3.1.2. Turbulent jet model. In the jet-driven turbulent model, Kelvin-Helmholtz instabilities along the jet/environmental boundary lead to the formation of a turbulent viscous mixing layer, through which the cloud molecular gas is entrained (*Cantó and Raga*, 1991; *Raga et al.*, 1993; *Stahler*, 1994; *Lizano and Giovanardi*, 1995; *Cantó et al.*, 2003, and references therein). The mixing layer grows both into the environment and into the jet, and eventually the whole flow becomes turbulent. Discussion of the few existing numerical studies that investigate how molecular outflows are created by a turbulent jet is presented in a recent review by *Raga et al.* (2004a), who cite the “Torino group” as the only simulations with predictions for atomic (e.g., H α , [SII]) emission (*Micono et al.*, 1998). The radiatively cooled jet simulations reproduce the broken power law behavior of the observationally determined mass-velocity distribution, even though molecular chemistry or cooling is not included (*Micono et al.*, 2000). However, these models produce decreasing molecular outflow momentum and velocity with distance from the powering source—opposite to that observed in most molecular outflows. An analytical model using Kelvin-Helmholtz instabilities has recently been proposed by *Watson et al.* (2004) to explain entrainment of cloud material by outflows from high-mass stars.

3.1.3. Jet bow shock model. In the jet-driven bow shock model, a highly collimated jet propagates into the surrounding ambient material, producing a thin outflow shell around the jet (*Raga and Cabrit*, 1993; *Masson and Chernin*, 1993). The physical origin of the jet is currently unclear and could even be considered as an extreme case of a highly collimated wide-angle wind without a tenuous wide-angle component. As the jet impacts the ambient material, a pair of shocks, a jet shock and a bow shock, are formed at the head of the jet. High pressure gas between the shocks is ejected sideways out of the jet beam, which then interacts with unperturbed ambient gas through a broader bow shock surface, producing an outflow shell surrounding the jet. An episodic variation in the mass-loss rate produces a chain of knotty shocks and bow shocks along the jet axis within the outflow shell. Recent analytical models without magnetic field include *Wilkin* (1996), *Zhang and Zheng* (1997), *Smith et al.* (1997), *Ostriker et al.* (2001), and *Downes and Cabrit* (2003).

There have been two recent sets of efforts (by two different groups) to model molecular protostellar jets numerically in two or three spatial dimensions, where the mass-velocity and position-velocity have routinely been measured. In these simulations, a tracer associated with molecular hy-

drogen is followed. However, each group approaches this problem in a different way, with each approach having its own advantages and disadvantages. In an effort to resolve the post-shock region, *Downes and Ray* (1999), and *Downes and Cabrit* (2003) have simulated relatively low density, axisymmetric (two-dimensional) fast jets. Alternatively, recognizing that observed flows associated with Class 0 sources have a higher density and a complex appearance, *Smith and Rosen* have extended the work of *Suttner et al.* (1997) and *Völker et al.* (1999) by further investigating sets of fully three-dimensional flows (e.g., *Rosen and Smith*, 2004a). The main disadvantage of this approach is that with such high densities the post-shock region will necessarily be under-resolved, especially in three-dimensional flows. Both the *Downes* and *Smith* groups have included molecular hydrogen dissociation and reformation as well as ro-vibrational cooling in their hydrodynamical simulations, although the treatment of this cooling is quite different in each group. One example is that the *Downes* group turns off all cooling and chemistry below 1000 K, while the *Smith and Rosen* simulations (explained in detail in *Smith and Rosen*, 2003) include cooling and chemistry calculations at essentially all temperatures (albeit with an equilibrium assumption for some reactions). The jet flows themselves enter the grid from a limited number of zones at one side of the computational domain, with densities and temperatures that are constant radially (a top hat profile) and over time. Both groups usually model the jet as nearly completely molecular—even though there are arguments suggesting that the jet will not initially be molecular, and that H₂ might subsequently form on the internal working surfaces of the jet (*Raga et al.*, 2005). The initial jet velocities of the *Downes*, and *Smith and Rosen* groups are varied with shear, pulsation, and, in the three dimensional simulations, with precession.

These different approaches have yielded different slopes for the computed CO intensity-velocity plots. The *Downes* group results have tended to be steeper and closer to the nominal value of $\gamma = 2$, while the standard *Rosen and Smith* case has a value near 1. Much of this difference can be attributed to the difference in jet-to-ambient density ratio (see *Rosen and Smith*, 2004a), which is 1 in the *Downes* standard case, and 10 in the *Rosen and Smith* standard case. The value of γ has been shown in these simulations to evolve over time, with steeper slopes associated with older flows. Most of these simulations are quite young, but there has been a recent effort to run the simulations out to $t = 2300$ yr (*Keegan and Downes*, 2005). They confirm the steepening of the mass-velocity slope up to $t = 1600$ yr (when $\gamma = 1.6$), and then it becomes roughly constant. The *Smith and Rosen* group have investigated whether fast (*Rosen and Smith*, 2004b) or slow (*Smith and Rosen*, 2005) precession has an effect on the mass-velocity slopes. While the simulations with fast precessing jets show a dependence of γ on the precession angle (generally increasing γ with the angle), some of this dependence was reduced in the slowly precessing cases. However, at this time only very young (t

< 500 yr) precessing sources have been simulated.

The initially molecular jet simulations that include periodic velocity pulses exhibit position-velocity plots with a sequence of Hubble wedges, similar to that observed in molecular outflows produced by an episodic protostellar wind (see Sec. 2.1.2). Where computed, velocity channel maps in CO from molecular jet simulations, as in *Rosen and Smith* (2004a), have a morphology similar to that of many sources (e.g., HH 211, *Gueth and Guilloteau*, 1999), i.e. revealing the knots within the jet at high velocities and showing the overall shape of the bow shock at low velocities.

Some recent studies show the need to expand the interpretation of molecular outflow observations beyond the simulated H₂ and CO emission from the numerical models discussed above. For example, the work of *Lesaffre et al.* (2004) includes more complex chemistry in one dimension, focusing on the unstable nature of combined C and J shocks. Also, radiation transfer with a complex chemistry has been simulated for a steady three dimensional (jet) flow, with a focus on HCO⁺ emission (*Rawlings et al.*, 2004).

In addition, magnetic field effects have been included in atomic protostellar jets that are axisymmetric (*Gardiner et al.*, 2000; *Stone and Hardee*, 2000) and fully three-dimensional (*Cerqueira and de Gouveia dal Pino*, 1999, 2001) and even molecular axisymmetric protostellar jets (*O’Sullivan and Ray*, 2000). These studies show significant differences compared to simulations of jets without magnetic fields. For example, magnetic tension, either along the jet axis or as a hoop stress from a toroidal field, can help collimate and stabilize the jet—though some of the additional stability is mitigated in a pulsed jet. Some of the differences between pure HD and MHD simulations that show up in the axisymmetric cases are less prominent in three dimensional simulations (*Cerqueira and de Gouveia dal Pino*, 2001).

3.1.4. Circulation models. In circulation models the molecular outflow is not entrained by an underlying wind or jet, it is rather formed by infalling matter that is deflected away from the protostar in a central torus of high MHD pressure through a quadrupolar circulation pattern around the protostar, and accelerated above escape speeds by local heating (*Fiege and Henriksen*, 1996a,b). The molecular outflow may still be affected by entrainment from the wind or jet, but this would be limited to the polar regions and it would not be the dominant factor for its acceleration (*Lery et al.*, 1999, 2002). Circulation models may provide a means of injecting added mass into outflows from O stars where it appears unlikely that direct entrainment can supply all the observed mass in the flow (*Churchwell*, 1999).

The most recent numerical studies of the circulation model have focused on a steady-state axisymmetric case, usually involving radiative heating, magnetic fields and Poynting flux (*Lery*, 2003). The addition of the Poynting flux in recent versions of this model has alleviated one of its major flaws (*Lery et al.*, 2002), i.e. the inability in earlier models to generate an outflow of sufficient speed. The toroidal magnetic field in what is currently being called the

“steady-state transit model” assists in the formation of a collimated fast moving flow (Combet et al., 2006).

3.2 Comparing Observations and Models

In the past ten years, molecular outflows have been mapped at high angular resolutions with millimeter interferometers, allowing us to confront the outflow models in great detail. A schematic of the predicted properties of molecular outflows produced by the different models discussed above is presented in Fig. 2. High-resolution molecular outflow observations can be used to compare the data with the outflow characteristics shown in Fig. 2 in order to establish what model best fits the observed outflow.

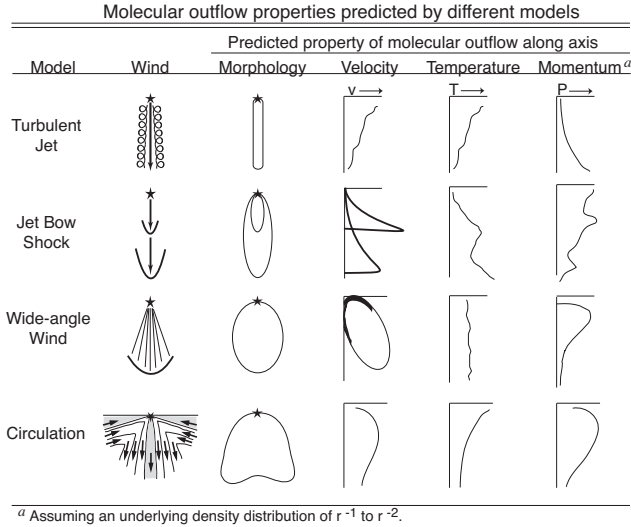


Fig. 2.— Observable molecular outflow properties predicted by the four leading broad classes of models: 1) turbulent jet (Cantó and Raga, 1991; Chernin and Masson, 1995; Bence et al., 1996); 2) jet bow shock (Chernin and Masson, 1995; Cliffe et al., 1996; Hatchell et al., 1999; Lee et al., 2001); 3) wide-angle wind (Li and Shu, 1996; Lee et al., 2001); and 4) circulation models (Fiege and Henriksen, 1996b; Lery et al., 1999). In the jet-driven bow shock model, an episodic variation in jet velocity produces an internal bow shock driving an internal shell, in addition to the terminal shock. This episodic variation can also be present in the other wind models, but in this figure the effects of an episodic wind are only shown for the jet bow shock model. This figure is based on Figure 1 of Arce and Goodman (2002b).

Here we focus our attention on comparing observations with the jet-driven bow shock and wide-angle wind-driven models, as most of the numerical simulations concentrate on these two models and they are the most promising models thus far. The predicted mass-velocity relationships in jet bow shock and wide-angle wind models have a slope (γ) of 1–4, in tune with observations. Each model predicts a somewhat different position-velocity (PV) relation that can be used to differentiate between these two leading molecular outflow driving mechanisms (Cabrit et al., 1997; Lee et al., 2000, 2001).

3.2.1. *Jet-driven bow shock models vs. observations.* Current jet-driven bow shock models can qualitatively account for the PV spur structure (where the outflow velocity increases rapidly toward the position of the internal and

leading bow shocks, see Fig. 2), the broad range of CO velocities near H_2 shocks, and the morphological relation between the CO and H_2 emission seen in young and collimated outflows. These models are able to produce the observed outflow width for highly collimated outflows, such as L 1448, HH 211 and HH 212 (Bachiller et al., 1995; Gueth and Guilloteau, 1999; Lee et al., 2001). However, jet-driven bow shock models have difficulty producing the observed width of poorly collimated outflows, like RNO 91, VLA 05487, and L 1221 (Lee et al., 2000, 2001, 2002). Jet models produce narrow molecular outflows mainly because the shocked gas in the bow shock working surfaces limits the transverse momentum (perpendicular to the jet-axis) that can be delivered to the ambient medium. In numerical simulations of jets, the width of the outflow shell is mainly determined by the effects of the leading bow shock from the jet’s first impact into the ambient material (e.g., Suttner et al., 1997; Downes and Ray, 1999; Lee et al., 2001). While the jet penetration into the cloud increases roughly linearly with time, the width only grows as the one-third power of time (Masson and Chernin, 1993; Wilkin, 1996; Ostriker et al., 2001).

Jets also have difficulty producing the observed outflow momenta. The transverse momentum of the outflow shell is acquired primarily near the jet head where the pressure gradient is large, and the mean transverse velocity of the shell, \bar{v}_R , can be approximated by $\bar{v}_R \simeq \beta c_s (R_j^2/R^2)$, where R and R_j are the outflow and jet radius, respectively, and βc_s is the velocity of the gas ejected from the working surface (Ostriker et al., 2001). For example, in a 10,000 AU-wide molecular outflow driven by a 150 AU jet, and assuming $\beta c_s = 32 \text{ km s}^{-1}$, the expected mean transverse velocity of the shell is only 0.03 km s^{-1} . As a result, if outflows were driven by a steady jet, the wide portions of outflow shells would exhibit extremely low velocities and very small momenta. This is inconsistent with the observations, especially in the wider flows where the well-defined cavity walls have appreciable velocities (e.g., B5-IRS1: Velusamy and Langer, 1998; RNO91: Lee et al., 2002; L1228: Arce and Sargent, 2004).

Systematic wandering of the jet flow axis has been argued to occur in several outflows based on outflow morphology, e.g., IRAS 20126+4104 (Shepherd et al., 2000) and L 1157 (Bachiller et al., 2001). This may mitigate the above discrepancies. The width and momentum of the outflow shell can increase because a wandering jet has a larger “effective radius” of interaction and can impact the outflow shell more directly (Raga et al., 1993; Cliffe et al., 1996). Some simulations show hints of widening by jet wandering (Völker et al., 1999; Rosen and Smith, 2004a; Smith and Rosen, 2005), but some show that a wandering jet could produce a smaller width than a steady jet (Raga et al., 2004b). Further calculations are needed to ascertain if motion of the jet axis at realistic levels can improve quantitative agreement with observed outflow features.

3.2.2. *Wide-angle wind models vs. observations.* Wide-angle winds can readily produce CO outflows with large

widths but have trouble producing other commonly observed features. In this model, the outflow velocity also increases with the distance from the source, showing a lobe PV structure tilted with inclination that exhibits only a small velocity range at the tip. If the tip is not observed, the PV structure appears as a tilted parabola (see Fig. 2). As discussed in Sec. 3.1.1, most wind-driven models, assume the protostellar wind density depends on the angle from the pole (θ). If the wind velocity has a small, or no, dependence on θ , and assuming a density stratification similar to that proposed by *Li and Shu* (1996), then the outflow width, W , can be expressed in terms of the ratio of wind to ambient density at the equator, (ρ_{wo}/ρ_{ao}) , the wind velocity at the pole, v_{wo} , and the outflow age, t , as $W \approx (\rho_{wo}/\rho_{ao})^{1/4} v_{wo} t$ (*Lee et al.*, 2001). For (ρ_{wo}/ρ_{ao}) between 10^{-3} and 10^{-4} , a 100 km s^{-1} wind can produce an outflow width of 0.1 to 0.2 pc in 10^4 years. Thus, the wind-driven model can produce widths consistent with observed molecular outflows in about 10^4 years. However, these models have problems producing discrete bow shock type features in the entrained molecular gas, as seen in many high-resolution maps of CO outflows (e.g., *Lee et al.*, 2000, 2002), and discrete position-velocity spur structures (and Hubble wedges). These features are hard to generate as the wide wind impacts all locations on the shell. Models of wide-angle pulsed winds produce a series of flat internal shocks within the outflow shell (*Lee et al.*, 2001), inconsistent with the curved internal H_2 bow shocks typically observed in episodic outflows (see Sec 2.1).

One possible solution to these problems is to require the winds to have a collimated core with a strong velocity gradient with respect to θ . A disk-wind driven from a large range of radii may have velocity strongly decreasing toward equatorial latitudes, because the asymptotic velocity on a given streamline in an MHD wind is characteristic of the Keplerian speed at the streamline’s footpoint (see chapter by *Pudritz et al.*). Further work is needed to study whether this sort of modification can produce the observed outflow features.

3.2.3. A synthesis with an evolutionary scenario. A model which combines attributes of the jet and wide-angle wind models is arguably the best match to the available CO outflow data. A two component protostellar wind may be produced, for example, by a slow disk wind and a fast central disk-driven jet or X-wind (arising from the magnetosphere-disk boundary region). The disk wind could help collimate the X-wind into the jet component (*Ostriker*, 1997) and provide a slow wide-angle component that drives the outflow width and momentum (see chapter by *Shang et al.*).

Observational support for the synthesis model exist at different wavelengths. There is mounting evidence from millimeter observations that the morphology of some molecular outflows is better explained with a “dual-wind” model (e.g., *Yu et al.*, 1999; *Arce and Goodman*, 2002a; *Arce and Sargent*, 2004). In the optical, the forbidden emission line profiles of T Tauri stars show two velocity

components: a high-velocity component that is argued to arise in a jet and a low-velocity component that might result from a disk-wind (*Kwan and Tademaru*, 1995; chapter by *Ray et al.*). A possible scenario is that the main driving agent producing most of the observed molecular outflow may change over the time, as discussed in Sec. 2. Numerical simulations of an evolving dual-wind model will be critical to study whether this proposed scenario can reproduce the wide range of observed features in molecular outflows from low- and high-mass protostars.

4. IMPACT OF OUTFLOWS ON SURROUNDING ENVIRONMENT

4.1 Physical Impact

Outflows from newborn stars inject momentum and energy into the surrounding molecular cloud at distances ranging from a few AU to up to tens of parsecs away from the source. Historically, most studies have concentrated on the interaction between the outflow and the surrounding core (~ 0.1 to 0.3 pc) as these scales can easily be observed with single-dish telescopes in the nearby ($\lesssim 1$ kpc) star forming regions. More recently, studies using millimeter interferometer array and single telescopes with focal-plane arrays have been crucial in the understanding of the outflow’s impact at smaller (< 0.1 pc) and larger ($\gtrsim 1$ pc) scales, respectively.

4.1.1. Outflow-envelope interactions. Protostellar winds originate within a few AU of the star (see chapter by *Ray et al.*), and so they are destined to interact with the dense circumstellar envelope—the primary mass reservoir of the forming star, with sizes in the range of 10^3 to 10^4 AU. In fact, survey studies of the circumstellar gas within 10^4 AU of low-mass YSOs show outflows contribute significantly to the observed mass-loss of the surrounding dense gas (from about 10^{-8} to $10^{-4} M_{\odot} \text{ yr}^{-1}$, depending on the protostar’s age) and indicate there is an evolution in the outflow-envelope interaction (e.g., *Fuller and Ladd*, 2002; *Arce and Sargent*, in preparation). As shown below, detailed studies of individual sources corroborate these results. The powerful outflows from low-mass class 0 sources are able to modify the distribution and kinematics of the dense gas surrounding a protostar, as evidenced in L 1157 (*Gueth et al.*, 1997; *Beltrán et al.*, 2004b), and RNO 43 (*Arce and Sargent*, 2005) where molecular line maps show the circumstellar high-density gas has an elongated structure and a velocity gradient, at scales of 4000 AU, along the outflow axis. Similarly, in IRAM 0491 (*Lee et al.*, 2005) and HH 212 (*Wiseman et al.*, 2001) the dense gas traced by N_2H^+ and NH_3 , respectively, exhibit blue- and red-shifted protrusions extending along the blue and red outflow lobes, evidence that there are strong outflow-envelope interactions in these class 0 sources. These results clearly show that, independent of the original (i.e., pre-protostellar outflow) underlying circumstellar matter distribution, young outflows entrain dense envelope gas along the outflow axis.

Although not as powerful as those of class 0 sources, the wide-angle outflows typically observed in class I sources (with opening angles of $\gtrsim 90^\circ$) are capable of constraining the infalling envelope to a limited volume outside the outflow lobes, as seen in the L 1228 (Arce and Sargent, 2004) and B5-IRS1 (Velusamy and Langer, 1998) outflows. The L1228 outflow is currently eroding the surrounding envelope by accelerating high-density ambient gas along the outflow-envelope interface and has the potential to further widen the cavities, as the outflow ram pressure is about a factor of 4 higher than the infall ram pressure (Arce and Sargent, 2004). In RNO 91, a class II source, the outflow exhibits an even wider opening angle of 160° that is expanding, and decreasing the volume of the infall region (Lee and Ho, 2005).

Widening of the outflow opening angle with age appears to be a general trend in low-mass protostars and there is ample evidence for erosion of the envelope due to outflow-envelope interactions (Velusamy and Langer, 1998; Arce and Sargent, 2004; Arce, 2004; Lee and Ho, 2005; Arce and Sargent, in preparation). Thus, it is clear that even if the pre-protostellar outflow circumstellar distribution of matter has a lower density along the polar regions (i.e., the outflow axis) as suggested by different models (i.e., Hartmann et al., 1996; Li and Shu, 1996), outflow-envelope interactions will have an impact on the subsequent circumstellar density distribution, as they will help widen the cavity and constrain the infall region. It is tempting to extrapolate and suggest that as a young star evolves further its outflow will eventually become wide enough to end the infall process and disperse the circumstellar envelope altogether.

4.1.2. Outflow-core interactions. Strong evidence exists for the disruptive effects outflows have on their parent core—the dense gas within 0.1 to 0.3 pc of the young star. Direct evidence of outflow-core interaction comes from the detection of velocity shifts in the core’s medium and high-density gas in the same sense, both in position and velocity, as the high-velocity (low-density) molecular outflow traced by ^{12}CO (e.g., Tafalla and Myers, 1997; Dobashi and Uehara, 2001; Takakuwa et al., 2003; Beltrán et al., 2004a). The high opacity of the ^{12}CO lines hampers the ability to trace low-velocity molecular outflows in high-density regions. Therefore, other molecular species like ^{13}CO , CS, C^{18}O , NH_3 , CH_3OH , and C_3H_2 are used to trace the high-density gas perturbed by the underlying protostellar wind. The average velocity shifts in the dense core gas are typically lower than the average velocity of the molecular (^{12}CO) outflow, consistent with a momentum-conserving outflow entrainment process. In addition to being able to produce systematic velocity shifts in the gas, outflows have been proposed to be a major source of the turbulence in the core (e.g., Myers et al., 1988; Fuller and Ladd, 2002; Zhang et al., 2005).

Outflows can also reshape the structure of the star-forming core by sweeping and clearing the surrounding dense gas and producing density enhancements along the outflow axis. The clearing process is revealed by the pres-

ence of nebular emission resulting from the scattering of photons, from the young star, off of cavity walls created by the outflow (e.g., Yamashita et al., 1989; Shepherd et al., 1998; Yu et al., 1999), or depressions along the outflow axis in millimeter molecular line maps of high density tracers (e.g., Moriarty-Schieven and Snell, 1988; White and Fridlund, 1992; Tafalla et al., 1997). Outflow-induced density enhancements (and shock-heated dust) in the core may be revealed by the dust continuum emission (e.g., Gueth et al., 2003; Beuther et al., 2004; Sollins et al., 2004). A change in the outflow axis direction with time, as observed in many sources (see chapter by Bally et al.) will allow an outflow to interact with a substantial volume of the core and be more disruptive on the dense gas than outflows with a constant axis (e.g., Shepherd et al., 2000; Arce and Goodman, 2002a). By accelerating and moving the surrounding dense gas, outflows can gravitationally unbind a significant amount of gas in the dense core thereby limiting the star formation efficiency of the dense gas (see Matzner and McKee, 2000).

The study of Fuente et al. (2002) shows that outflows appear to be the dominant mechanism able to efficiently sweep out about 90% of the parent core by the end of the pre-main sequence phase of young intermediate-mass (Herbig Ae/Be) stars. In addition, outflows from low- and high-mass protostars have kinetic energies comparable to the gravitational binding energy of their parent core, suggesting outflows have the potential to disperse the entire core (e.g., Tafalla and Myers, 1997; Tafalla et al., 1997). We may even be observing the last stages of the outflow-core interaction in G192.16, a massive (early B) young star, where the dense core gas is optically thin and clumpy, and the ammonia core is gravitationally unstable (Shepherd et al., 2004). However, further systematic observations of a statistical sample of outflow-harboring cores at different ages are needed in order to fully understand the details of the core dispersal mechanism and conclude whether outflows can disperse their entire parent core.

Theoretical studies indicate that shocks from a protostellar wind impacting on a dense clump of gas (i.e., a pre-stellar core) along the outflow’s path can trigger collapse and accelerate the infall process in the impacted core (Foster and Boss, 1996; Motoyama and Yoshida, 2003). Outflow-triggered star-formation has been suggested in only a handful of sources where the morphology and velocity structure of the dense gas surrounding a young protostar appears to be affected by the outflow from a nearby YSO (Girart et al., 2001; Sandell and Knee, 2001; Yokogawa et al., 2003).

4.1.3. Outflow-cloud interactions far from the source. Giant outflows from young stars of all masses are common, and they can interact with the cloud gas at distances greater than 1 pc from their source (Reipurth et al., 1997; Stanke et al., 2000). Outflows from low-mass protostars are able to entrain 0.1 to 1 M solar masses of cloud material, accelerate and enhance the linewidth of the cloud gas (Bence et al., 1996; Arce and Goodman, 2001b), and in some cases their

kinetic energy is comparable to (or larger than) the turbulent energy and gravitational binding energy of their parent cloud (Arce, 2003). The effects of giant outflows from intermediate- and high-mass YSOs on their surroundings can be much more damaging to their surrounding environment. Studies of individual sources indicate that giant outflows are able to entrain tens to hundreds of solar masses, induce parsec-scale velocity gradients in the cloud, produce dense massive shells of swept-up gas at large (> 0.5 pc) distances from the source, and even break the cloud apart (Fuente et al., 1998; Shepherd et al., 2000; Arce and Goodman, 2002a; Benedettini et al., 2004). The limited number of studies in this field suggest that a single giant outflow has the *potential* to have a disruptive effect on their parent molecular cloud (e.g., Arce, 2003). Clearly, additional observations of giant outflows and their clouds are needed in order to quantify their disruptive potential.

Most star formation appears in a clustered mode and so multiple outflows should be more disruptive on their cloud than a single star. Outflows from a group of young stars interact with a substantial volume of their parent cloud by sweeping up the gas and dust into shells (e.g., Davis et al., 1999; Knee and Sandell, 2000), and may be a considerable, albeit not the major, source of energy for driving the supersonic turbulent motions inside clouds (Yu et al., 2000; Williams et al., 2003; Mac Low and Klessen, 2004). It has also been suggested that past outflow events from a group of stars may leave their imprint on the cloud in the form of numerous cavities (e.g., Bally et al., 1999; Quillen et al., 2005). Very limited (observational and theoretical) work on this topic exists, and further observations of star forming regions with different environments and at different evolutionary stages are essential to understand the role of outflows in the gaseous environs of young stellar clusters.

4.2 Shock chemistry

The propagation of a supersonic protostellar wind through its surrounding medium happens primarily via shock waves. The rapid heating and compression of the region trigger different microscopic processes —such as molecular dissociation, endothermic reactions, ice sublimation, and dust grain disruption— which do not operate in the unperturbed gas. The time scales involved in the heating and in some of the “shock chemistry” processes are short (a few 10^2 to 10^4 yr), so the shocked region rapidly acquires a chemical composition distinct from that of the quiescent unperturbed medium. Given the short shock cooling times ($\sim 10^2$ yr, Kaufman and Neufeld, 1996), some of these high-temperature chemical processes only operate at the initial stages, as the subsequent chemical evolution is dominated by low temperature processes. This chemical evolution, the gradual clearing of the outflow path, and the likely intrinsic weakening of the main accelerating agent, all together make the important signatures of the shock interaction (including some of the chemical anomalies) vanish as the protostellar object evolves. Chemical anomalies found in an outflow

can therefore be considered as an indicator of the outflow age (e.g., Bachiller et al., 2001).

The chemical impact of outflows are better studied in outflows around Class 0 sources with favorable orientation in the sky (i.e., high inclination with respect to the line of sight). With less confusion than that found around massive outflows, the shocked regions of low-mass, high-collimation outflows (which often adopt the form of well-defined bows) are well separated spatially with respect to the quiescent gas. Detail studies of these “simple” regions can help disentangle the effects of outflow shocks from other shocks in more complex regions — like in circumstellar disks, where one expects to find outflow shock effects blended with those produced by shocks triggered by the collapsing envelope (e.g., Ceccarelli et al., 2000).

Shocks in molecular gas can be of C-type or of J-type, depending on whether the hydrodynamical variables change continuously across the shock front (e.g., Draine and McKee, 1993). C-shocks are mediated by magnetic fields acting on ions that are weakly coupled with neutrals, they are slow, have maximum temperatures of about 2000-3000 K, and are non-dissociative. J-shocks are typically faster, and can reach much higher temperatures. The critical velocity at which the change between C- and J-regime is produced depends on several parameters such as the pre-shock density (Le Bourlot et al., 2002) and the presence of charged grains (Flower and Pineau des Forêts, 2003), and it typically ranges from ~ 20 up to ~ 50 km s $^{-1}$. J-shocks may also occur at relatively low velocities when the transverse component of the magnetic field is small (Flower et al., 2003). Recent infrared observations of several lines of H $_2$, CO, H $_2$ O, and OH, and of some crucial atomic lines, have made possible the estimate of temperature and physical conditions in a relatively large sample of outflows. It follows that the interpretation of the data from most shocked regions require a combination of C- and J-shocks (see Noriega-Crespo, 2002; van Dishoeck, 2004, for comprehensive reviews). Such a combination of shocks can be obtained by the overlap of multiple outflow episodes as observed in several sources, and/or by the bow shock geometry which could generate J-shocks at the apex of the bow together with C-shocks at the bow flanks (Nisini et al., 2000; O’Connell et al., 2004, 2005). C-shocks are particularly efficient in triggering a distinct molecular chemistry in the region in which the molecules are preserved and heated to ~ 2000 -3000 K. Moreover, molecules can also reform in J-shocked regions when the gas rapidly cools, or in warm layers around the hottest regions. The main processes expected to dominate this shock chemistry were discussed by Richer et al. (2000).

Comprehensive chemical surveys have been carried out in two prototypical Class 0 sources (L1157: Bachiller and Pérez-Gutiérrez, 1997; BHR71: Garay et al., 1998). More recent observations, including high-resolution molecular maps, have been made for a sample of sources, for example: L1157 (Bachiller et al., 2001), NGC1333 IRAS2 (Jørgensen et al., 2004), NGC1333 IRAS 4 (Choi et al.,

2004), NGC2071 (*Garay et al.*, 2000), Cep-A (*Codella et al.*, 2005). These observations have revealed that there are important differences in molecular abundances in different outflow regions. Such variations in the abundances may be linked to the time evolution of the chemistry (*Bachiller et al.*, 2001) and may also be related to variations in the abundance of the atomic carbon (*Jørgensen et al.*, 2004).

SiO exhibits the most extreme enhancement factors (up to $\sim 10^6$) with respect to the quiescent unperturbed medium. Such high enhancements are often found close to the heads (bowshocks), and along the axes, of some highly collimated outflows (e.g., *Dutrey et al.*, 1997, and references therein; *Codella et al.*, 1999; *Bachiller et al.*, 2001; *Garay et al.*, 2002; *Jørgensen et al.*, 2004; *Palau et al.*, 2006, and references therein). Sputtering of atomic Si from the dust grains is at the root of such high SiO abundances (*Schilke et al.*, 1997), a process which requires shock velocities in excess of $\sim 25 \text{ km s}^{-1}$. Accordingly, the SiO lines usually present broad wings and, together with CO, the SiO emission usually reaches the highest terminal velocities among all molecular species. Moreover, recent observations of several outflows have revealed the presence of a narrow ($< 1 \text{ km s}^{-1}$) SiO line component (*Lefloch et al.*, 1998; *Codella et al.*, 1999; *Jiménez-Serra et al.*, 2004). The presence of SiO at low velocities is not well understood. Plausible explanations include that this is the signature of a shock precursor component (*Jiménez-Serra et al.*, 2004, 2005) or that SiO is indeed produced at high velocities and subsequently slowed down in time scales of $\sim 10^4 \text{ yr}$ (*Codella et al.*, 1999).

CH₃OH and H₂CO are also observed to be significantly overabundant in several outflows, enhanced by factors of about 100 (*Bachiller et al.*, 2001; *Garay et al.*, 2000; *Garay et al.*, 2002; *Jørgensen et al.*, 2004; *Maret et al.*, 2005). These two species are likely evaporated directly from the icy dust mantles, and in many cases the terminal velocities of their line profile wings are significantly lower than that of SiO, probably because CH₃OH and H₂CO do not survive at velocities as high as those required to form SiO (*Garay et al.*, 2000). Thus, an enhancement of CH₃OH and H₂CO with no SiO may indicate the existence of a weak shock. On the other hand, after the passage of a strong shock, and once the abundances of CH₃OH, H₂CO and SiO are enhanced in the gas phase, one would expect the SiO molecules to re-incorporate to the grains while some molecules of CH₃OH and H₂CO remain in the gas-phase, as these two molecules are more volatile than SiO (their molecular depletion timescales are about a few 10^3 yr for densities of $\sim 10^6 \text{ cm}^{-3}$). In this scenario enhancement of CH₃OH and H₂CO most likely may mark a later stage in the shock evolution than that traced by high SiO abundances.

In several outflows HCO⁺ high velocity emission is only prominent in regions of the outflow which are relatively close to the driving sources (*Bachiller et al.*, 2001; *Jørgensen et al.*, 2004). In such regions, the HCO⁺ abundance can be enhanced by a factor of ~ 20 . This behavior can be understood if the HCO⁺ that was originally pro-

duced through shock-induced chemistry (e.g., *Rawlings et al.*, 2004) is destroyed by dissociative recombination or by reaction with the abundant molecules of H₂O (*Bergin et al.*, 1998). Once the abundance of the gaseous H₂O decreases due to freeze-out, the abundance of HCO⁺ may increase. A rough anti-correlation between CH₃OH and HCO⁺ (*Jørgensen et al.*, 2004) seems to support these arguments. In other cases, HCO⁺ emission is observed at positions close to HH objects that can be relatively distant from the driving sources. In fact, together with NH₃, HCO⁺ is expected to be enhanced in clumps within the molecular cloud by UV irradiation from bright HH objects (*Viti and Williams*, 1999), an effect observed near HH2 according to *Girart et al.* (2002). Nevertheless, *Girart et al.* (2005) have recently found that UV irradiation alone is insufficient to explain the measured HCO⁺ enhancements and that strong heating (as that caused by a shock) is also needed.

The chemistry of sulfur bearing species is of special interest as it has been proposed to be a potential tool to construct chemical clocks to date outflows (and hence their protostellar driving sources). The scenario initially proposed by a number of models is that H₂S is the main reservoir of S in grain mantles, although recent observations seem to indicate that OCS is more abundant on ices than H₂S (*Palumbo et al.*, 1997; *van der Tak et al.*, 2003). Once H₂S is ejected to the gas phase by the effect of shocks, its abundance will rapidly decrease after 10^4 yr (e.g., *Charnley*, 1997) due to oxidation with O and OH, thereby producing SO (first) and SO₂ (at a later time). Models and observations indicate that the SO/H₂S and SO₂/H₂S ratios are particularly promising for obtaining the relative age of shocks in an outflow (*Charnley*, 1997; *Hatchell et al.*, 1998; *Bachiller et al.*, 2001; *Buckle and Fuller*, 2003). On the other hand, recent models by *Wakelam et al.* (2004) have shown that the chemistry of sulfur can be more complex than previously thought since — among other reasons — the abundances of the sulfur-bearing species critically depend on the gas excitation conditions, which in turn depend on the outflow velocity structure. *Wakelam et al.* (2005) used the SO₂/SO and the CS/SO ratios to constrain the age of the NGC1333 IRAS2 outflow to $\leq 5 \times 10^3 \text{ yr}$. A recent study by *Codella et al.* (2005) confirms that the use of the SO/H₂S and SO₂/H₂S ratios is subject to important uncertainties in many circumstances, and that other molecular ratios (e.g., CH₃OH/H₂CS, OCS/H₂CS) can be used as more effective chemical clocks to date outflows.

Recent work has revealed that chemical studies can be useful for the investigation of interstellar gas structure. For instance, *Viti et al.* (2004) have recently shown that, if the outflow chemistry is dominated by UV irradiation, clumping in the surrounding medium prior to the outflow passage is needed in order to reproduce the observed chemical abundances in some outflows. We stress, however, that this result depends on the chemical modeling and that more work is needed before it can be generalized.

5. FUTURE WORK

We discussed how the high angular resolution observations have revealed general properties and evolutionary trends in molecular outflows from low- and high-mass protostars. However, these results rely on a limited number of outflows maps, thus making any statistical analysis somewhat dangerous. A large sample of fully mapped outflows at different evolutionary stages, using millimeter interferometers, is needed to soundly establish an empirical model of outflow evolution, and the outflow's physical and chemical impact on its surroundings. Also, detail mapping of many outflows will enable a thorough comparison with different numerical outflow models in order to study the outflow entrainment process.

Further progress in our understanding of outflows is expected from current or planned instrument developments that aim at improving both the sensitivity and the angular resolution, while opening new frequency windows. The soon to be implemented improvements to the IRAM Plateau de Bure interferometer — which include longer baselines, wider frequency coverage, and better sensitivity — as well as the soon to be operational Combined Array for Research in Millimeter-wave Astronomy (CARMA) will allow multi-line large-scale mosaic maps with 1" resolution (or less), required to thoroughly study the outflow physical properties (e.g., kinematics, temperature, densities), the entrainment process and the different chemical processes along the outflows' entire extent. In addition, large-scale mosaic maps of clouds with outflows will allow the study of the impact of many outflows on their parent cloud. The Atacama Large Millimeter Array (ALMA), presumably operational by 2012, will have the ability to determine high-fidelity kinematics and morphologies of even the most distant outflows in our Galaxy as well as flows in near-by galaxies. The superb (sub-arcsecond) angular resolution will be particularly useful to study how outflows are ejected from accretion disks, how molecular gas is entrained in the outflow, and the interaction between the molecular jet/outflow and the environment very close to the protostar (i.e., the infalling envelope, and protoplanetary disk). The Expanded Very Large Array (EVLA), expected to be complete in 2012, will be critical to image the wide-opening angle, ionized outflow close to the powering source, and will allow sensitive studies of re-ionization events in jets, H₂O masers and SiO(1–0) in outflows.

New submillimeter facilities and telescopes under construction will soon provide sensitive observations of high excitation lines, important for the study of outflow driving and entrainment, as well as shock-induced chemical processes. The recently dedicated Submillimeter Array (SMA) is the first instrument capable of studying the warm molecular gas in the CO(6–5) line, at (sub)arcsecond resolution, allowing to trace the outflow components closer to the driving source and closer to the jet axis than previously possible. Furthermore, the large bandwidth of the correlator allows for simultaneous multi-line observations crucial for study-

ing the various shock chemistry processes in the outflow. Also, the Herschel Space Observatory (HSO) will measure the abundances of shock tracers of great interest, in particular water, which cannot be observed from the ground.

In the near future, greater computing power will make possible larger scale numerical simulations that take advantage of adaptive grids, better and more complex cooling and chemistry functions, and the inclusion of radiative transfer and magnetic fields. Given the wealth of high-resolution data that will soon be available, numerical studies will need to compare the simulated outflows with observations in more detail, using the outflow density, kinematics, temperature and chemical structure. In addition, simulations that run for far longer times ($\sim 10^4 - 10^5$ yr) than current models ($\sim 10^3$ yr) are needed to study the outflow temporal behavior and evolution. Advances in computing, perhaps including GRID technology, may even allow a version of a virtual telescope, where both numerical modelers and observers can find the best fit from a set of models for different sources.

Acknowledgments. H.G.A. is supported by an NSF Astronomy and Astrophysics Postdoctoral Fellowship under award AST-0401568. D.S. is supported by the National Radio Astronomy Observatory, a facility of the National Science Foundation operated under cooperative agreement by Associated Universities, Inc. R.B. acknowledges partial support from Spanish grant AYA2003-7584. A.R. acknowledges the support of the Visitor Theory Grant at Armagh Observatory, which hosted the author while some of the review was written. H.B. acknowledges financial support by the Emmy-Noether-Program of the Deutsche Forschungsgemeinschaft (DFG, grant BE2578).

REFERENCES

- Anglada G., Estalella R., Rodríguez L. F., Torrelles J. M., Lopez R., and Cantó, J. (1991) *Astrophys. J.*, 376, 615-617.
- Arce H. G. (2003) *Rev. Mexicana Astron. Astrofis. Conf. Series*, 15, 123-125.
- Arce H. G. (2004) In *IAU Symp. 221: Star Formation at High Angular Resolution* (M. Burton et al., eds.) pp. 345-350. Kluwer, Dordrecht.
- Arce H. G. and Goodman A. A. (2001a) *Astrophys. J.*, 551, L171-L174.
- Arce H. G. and Goodman A. A. (2001b) *Astrophys. J.*, 554, 132-151.
- Arce H. G. and Goodman A. A. (2002a) *Astrophys. J.*, 575, 911-927.
- Arce H. G. and Goodman A. A. (2002b) *Astrophys. J.*, 575, 928-949.
- Arce H. G. and Sargent A. I. (2004) *Astrophys. J.*, 612, 342-356.
- Arce H. G. and Sargent A. I. (2005) *Astrophys. J.*, 624, 232-245.
- Avery L. W., Hayashi S. S., and White G. L. (1990) *Astrophys. J.*, 357, 524-530.
- Bachiller R. and Tafalla M. (1999) In *The Origin of Stars and Planetary System* (C. J. Lada and N. D. Kylafis, eds.), pp. 227-265. Kluwer, Dordrecht.

- Bachiller R., Martín-Pintado J., Tafalla M., Cernicharo J., and Lazareff B. (1990) *Astron. Astrophys.*, 231, 174-186.
- Bachiller R., Guilloteau S., Dutrey A., Planesas P., and Martín-Pintado J. (1995) *Astron. Astrophys.*, 299, 857-868.
- Bachiller R. and Pérez-Gutiérrez M. (1997) *Astrophys. J.*, 487, L93-L96.
- Bachiller R., Guilloteau S., Gueth F., Tafalla M., Dutrey A., Codella C., and Castets A. (1998) *Astron. Astrophys.*, 339, L49-L52.
- Bachiller R., Gueth F., Guilloteau S., Tafalla M., and Dutrey A. (2000) *Astron. Astrophys.*, 362, L33-L36.
- Bachiller R., Pérez-Gutiérrez M., Kumar M. S. N., and Tafalla M. (2001) *Astron. Astrophys.*, 372, 899-912.
- Bally J. and Lada C. J. (1983) *Astrophys. J.*, 265, 824-847.
- Bally J., Reipurth B., Lada C. J., and Billawala Y. (1999) *Astron. J.*, 117, 410-428.
- Beltrán M. T., Girart J. M., Estalella R., and Ho P. T. P. (2004a) *Astron. Astrophys.*, 426, 941-949.
- Beltrán M. T., Gueth F., Guilloteau S., and Dutrey A. (2004b) *Astron. Astrophys.*, 416, 631-640.
- Bence S. J., Richer J. S., and Padman R. (1996) *Mon. Not. R. Astron. Soc.*, 279, 866-883.
- Benedettini M., Molinari S., Testi L., and Noriega-Crespo A. (2004) *Mon. Not. R. Astron. Soc.*, 347, 295-306.
- Bergin E. A., Neufeld D. A., and Melnick G. J. (1998) *Astrophys. J.*, 499, 777-792.
- Beuther H. and Shepherd, D. S. (2005) In *Cores to Clusters: Star Formation with Next Generation Telescopes* (M.S.N. Kumar et al., eds.), pp. 105-119. Springer, New York.
- Beuther H., Schilke P., Sridharan T. K., Menten K. M., Walmsley C. M., et al. (2002a) *Astron. Astrophys.*, 383, 892-904.
- Beuther H., Schilke P., Gueth F., McCaughrean M., Andersen M., et al. (2002b) *Astron. Astrophys.*, 387, 931-943.
- Beuther H., Schilke P., and Gueth F. (2004) *Astrophys. J.*, 608, 330-340.
- Bonnell I. A., Bate M. R., and Vine S. G. (2003) *Mon. Not. R. Astron. Soc.*, 343, 413-418.
- Bontemps S., André P., Terebey S., and Cabrit S. (1996) *Astron. Astrophys.*, 311, 858-872.
- Buckle J. V. and Fuller G. A. (2003) *Astron. Astrophys.*, 399, 567-581.
- Cabrit S. and Bertout C. (1992) *Astron. Astrophys.*, 311, 858-872.
- Cabrit S., Raga A., and Gueth F. (1997) In *IAU Symp. 182: Herbig-Haro Flows and the Birth of Stars* (B. Reipurth and C. Bertout, eds.) pp. 163-180. Kluwer, Dordrecht.
- Cantó J. and Raga A. C. (1991) *Astrophys. J.*, 372, 646-658.
- Cantó J., Raga A. C., and Riera A. (2003) *Rev. Mexicana Astron. Astrofis.*, 39, 207-212.
- Ceccarelli C., Castets A., Caux E., Hollenbach D., Loinard L., et al. (2000) *Astron. Astrophys.*, 355, 1129-1137.
- Cernicharo J., Neri R., and Reipurth B. (1999) In *IAU Symp. 182: Herbig-Haro Flows and the Birth of Low Mass Stars* (B. Reipurth and C. Bertout, eds.), pp. 141-152. Kluwer, Dordrecht.
- Cerqueira A. H. and de Gouveia dal Pino E. M. (1999) *Astrophys. J.*, 510, 828-845.
- Cerqueira A. H. and de Gouveia dal Pino E. M. (2001) *Astrophys. J.*, 560, 779-791.
- Cesaroni R. (2005) *Astrophys. Space Sci.*, 295, 5-17.
- Cesaroni R., Felli M., Jenness T., Neri R., Olmi L., et al. (1999) *Astron. Astrophys.*, 345, 949-964.
- Chandler C. J. and Richer J. S. (2001) *Astrophys. J.*, 555, 139-145.
- Charnley S. B. (1997) *Astrophys. J.*, 481, 396-405.
- Chernin L. M. and Masson C. R. (1995) *Astrophys. J.*, 455, 182-189.
- Choi M. (2005) *Astrophys. J.*, 630, 976-986.
- Choi M., Kamazaki T., Tatematsu K., and Panis J. F. (2004) *Astrophys. J.*, 617, 1157-1166.
- Churchwell E. (1999) In *The Origin of Stars and Planetary Systems* (C. J. Lada and N. D. Kylafis, eds.) pp. 515-552. Kluwer, Dordrecht.
- Cliffe J. A., Frank A., and Jones T. W. (1996) *Mon. Not. R. Astron. Soc.*, 282, 1114-1128.
- Codella C., Bachiller R., and Reipurth B. (1999) *Astron. Astrophys.*, 343, 585-598.
- Codella C., Bachiller R., Benedettini M., Caselli P., Viti S., and Wakelam V. (2005) *Mon. Not. R. Astron. Soc.*, 361, 244-258.
- Combet C., Lery T., and Murphy G. C. (2006) *Astrophys. J.*, 637, 798-810.
- Cunningham A., Frank A., and Hartmann L. (2005) *Astrophys. J.*, 631, 1010-1021.
- Davis C. J., Matthews H. E., Ray T. P., Dent W. R. F., and Richer J. S. (1999) *Mon. Not. R. Astron. Soc.*, 309, 141-152.
- Davis C. J., Varricatt W. P., Todd S. P., and Ramsay Howat S. K. (2004) *Astron. Astrophys.*, 425, 981-995.
- Delamarter G., Frank A., and Hartmann L. (2000) *Astrophys. J.*, 530, 923-938.
- Dobashi K. and Uehara H. (2001) *PASJ*, 53, 799-809.
- Downes T. P. and Cabrit S. (2003) *Astron. Astrophys.*, 403, 135-140.
- Downes T. P. and Ray T. P. (1999) *Astron. Astrophys.*, 345, 977-985.
- Draine B. T. and McKee C. F. (1993) *Ann. Rev. Astron. Astrophys.*, 31, 373-432.
- Dutrey A., Guilloteau S., and Bachiller R. (1997) *Astron. Astrophys.*, 325, 758-768.
- Eisloffel J., Smith M. D., Christopher J., and Ray T. P. (1996) *Astron. J.*, 112, 2086-2093.
- Fendt C. and Cemeljic M. (2002) *Astron. Astrophys.*, 395, 1045-1060.
- Fiege J. D. and Henriksen R. N. (1996a) *Mon. Not. R. Astron. Soc.*, 281, 1038-1054.
- Fiege J. D. and Henriksen R. N. (1996b) *Mon. Not. R. Astron. Soc.*, 281, 1055-1072.
- Flower D. R. and Pineau des Forêts G. (2003) *Mon. Not. R. Astron. Soc.*, 343, 390-400.
- Flower D. R., Le Bourlot J., Pineau des Forêts G., and Cabrit S. (2003) *Astrophys. Space Sci.*, 287, 183-186.
- Foster P. N. and Boss A. P. (1996) *Astrophys. J.*, 468, 784-796.
- Fuente A., Martín-Pintado J., Rodríguez-Franco A., and Moriarty-Schieven G. D. (1998) *Astron. Astrophys.*, 339, 575-586.
- Fuente A., Martín-Pintado J., Bachiller R., Rodríguez-Franco A., and Palla F. (2002) *Astron. Astrophys.*, 387, 977-992.
- Fuller G. A. and Ladd E. F. (2002) *Astrophys. J.*, 573, 699-719.
- Garay G., Köhnenkamp I., Bourke T. L., Rodríguez L. F., and Lehtinen K. K. (1998) *Astrophys. J.*, 509, 768-784.
- Garay G. and Lizano S. (1999) *PASP*, 111, 1049-1087.
- Garay G., Mardones D., and Rodríguez L. F. (2000) *Astrophys. J.*, 545, 861-873.
- Garay G., Mardones D., Rodríguez L. F., Caselli P., and Bourke T. L. (2002) *Astrophys. J.*, 567, 980-998.
- Gardiner T. A., Frank A., Jones T. W., and Ryu D. (2000) *Astrophys. J.*, 530, 834-850.
- Gardiner T. A., Frank A., and Hartmann L. (2003) *Astrophys. J.*,

- 582, 269-276.
- Gibb A. G., Richer J. S., Chandler C. J., and Davis C. J. (2004) *Astrophys. J.*, 603, 198-212.
- Girart J. M., Estalella R., Viti S., Williams D. A., and Ho P. T. P. (2001) *Astrophys. J.*, 562, L91-L94.
- Girart J. M., Viti S., Williams D. A., Estalella R., and Ho P. T. P. (2002) *Astron. Astrophys.*, 388, 1004-1015.
- Girart J. M., Viti S., Estalella R., and Williams D. A. (2005) *Astron. Astrophys.*, 439, 601-612.
- Gómez J. F., Sargent A. I., Torrelles J. M., Ho P. T. P., Rodríguez L. F., et al. (1999) *Astrophys. J.*, 514, 287-295.
- Greenhill L. J., Gwinn C. R., Schwartz C., Moran J. M., and Diamond P. J. (1998) *Nature*, 396, 650-653.
- Gueth F. and Guilloteau S. (1999) *Astron. Astrophys.*, 343, 571-584.
- Gueth F., Guilloteau S., and Bachiller, R. (1996) *Astron. Astrophys.*, 307, 891-897.
- Gueth F., Guilloteau S., Dutrey A., and Bachiller R. (1997) *Astron. Astrophys.*, 323, 943-952.
- Gueth F., Guilloteau S., and Bachiller R. (1998) *Astron. Astrophys.*, 333, 287-297.
- Gueth F., Schilke P., and McCaughrean M. J. (2001) *Astron. Astrophys.*, 375, 1018-1031.
- Gueth F., Bachiller R., and Tafalla M. (2003) *Astron. Astrophys.*, 401, L5-L8.
- Hartmann L., Calvet N., and Boss A. (1996) *Astrophys. J.*, 464, 387-403.
- Hatchell J., Thompson M. A., Millar T. J., and MacDonald, G. H. (1998) *Astron. Astrophys.*, 338, 713-722.
- Hatchell J., Fuller G. A., and Ladd E. F. (1999) *Astron. Astrophys.*, 344, 687-695.
- Hirano N., Liu S.-Y., Shang H., Ho P. T. P., Huang H.-C., et al. (2006) *Astrophys. J.*, 636, L141-L144.
- Jiménez-Serra I., Martín-Pintado J., Rodríguez-Franco A., and Marcelino N. (2004) *Astrophys. J.*, 603, L49-L52.
- Jiménez-Serra I., Martín-Pintado J., Rodríguez-Franco A., and Martín S. (2005) *Astrophys. J.*, 627, L121-L124.
- Jørgensen J. K., Hogerheijde M. R., Blake G. A., van Dishoeck E. F., Mundy L. G., and Schöier F. L. (2004) *Astron. Astrophys.*, 416, 1021-1037.
- Kaufman M. J. and Neufeld D. A. (1996) *Astrophys. J.*, 456, 611-630.
- Keegan R. and Downes T. P. (2005) *Astron. Astrophys.*, 437, 517-524.
- Knee L. B. G. and Sandell G. (2000) *Astron. Astrophys.*, 361, 671-684.
- Königl A. (1999) *New A Rev.*, 43, 67-77.
- Kwan J. and Tadamaru E. (1995) *Astrophys. J.*, 454, 382-393.
- Lada C. J. and Fich M. (1996) *Astrophys. J.*, 459, 638-652.
- Ladd E. F. and Hodapp K. W. (1997) *Astrophys. J.*, 474, 749-759.
- Le Boulrot J., Pineau des Forêts G., Flower D. R., and Cabrit S. (2002) *Mon. Not. R. Astron. Soc.*, 332, 985-993.
- Lee C.-F. and Ho P. T. P. (2005) *Astrophys. J.*, 624, 841-852.
- Lee C.-F., Mundy L. G., Reipurth B., Ostriker E. C., and Stone J. M. (2000) *Astrophys. J.*, 542, 925-945.
- Lee, C.-F., Stone J. M., Ostriker E. C., and Mundy L. G. (2001) *Astrophys. J.*, 557, 429-442.
- Lee C.-F., Mundy L. G., Stone J. M., and Ostriker E. C. (2002) *Astrophys. J.*, 576, 294-312.
- Lee C.-F., Ho P. T. P., and White S. M. (2005) *Astrophys. J.*, 619, 948-958.
- Lefloch B., Castets A., Cernicharo J., and Loinard L. (1998) *Astrophys. J.*, 504, L109-L112.
- Lery T. (2003) *Astrophys. Space Sci.*, 287, 35-38.
- Lery T., Henriksen R. N., and Fiege J. D. (1999) *Astron. Astrophys.*, 350, 254-274.
- Lery T., Henriksen R. N., Fiege J. D., Ray T. P., Frank A., and Bacciotti F. (2002) *Astron. Astrophys.*, 387, 187-200.
- Lesaffre P., Chièze J.-P., Cabrit S., and Pineau des Forêts G. (2004) *Astron. Astrophys.*, 427, 147-155.
- Li Z.-Y. and Shu F. H. (1996) *Astrophys. J.*, 472, 211-224.
- Lizano S. and Giovanardi C. (1995) *Astrophys. J.*, 447, 742-751.
- Mac Low M.-M. and Klessen R. (2004) *Rev. Modern Phys.*, 76, 125-196.
- Maret S., Ceccarelli C., Tielens A. G. G. M., Caux E., Lefloch B., et al. (2005) *Astron. Astrophys.*, 442, 527-538.
- Martín-Pintado J., Bachiller R., and Fuente A. (1992) *Astron. Astrophys.*, 254, 315-326.
- Martí J., Rodríguez L. F., and Reipurth B. (1993) *Astrophys. J.*, 416, 208-217.
- Masson C. R. and Chernin L. M. (1993) *Astrophys. J.*, 414, 230-241.
- Matzner C. D. and McKee C. F. (1999) *Astrophys. J.*, 526, L109-L112.
- Matzner C. D. and McKee C. F. (2000) *Astrophys. J.*, 545, 364-378.
- McCaughrean M. J. and Mac Low, M.-M. (1997) *Astron. J.*, 113, 391-400.
- Micono M., Massaglia S., Bodo G., Rossi P., and Ferrari A. (1998) *Astron. Astrophys.*, 333, 1001-1006.
- Micono M., Bodo G., Massaglia S., Rossi P., and Ferrari A. (2000) *Astron. Astrophys.*, 364, 318-326.
- Moriarty-Schieven G. H. and Snell R. L. (1988) *Astrophys. J.*, 332, 364-378.
- Moscadelli L., Cesaroni R., and Rioja M. J. (2005) *Astron. Astrophys.*, 438, 889-898.
- Motoyama, K. and Yoshida T. (2003) *Mon. Not. R. Astron. Soc.*, 344, 461-467.
- Myers P. C., Heyer M., Snell R. L., and Goldsmith P. F. (1988) *Astrophys. J.*, 324, 907-919.
- Nisini B., Benedettini M., Giannini T., and Codella C. (2000) *Astron. Astrophys.*, 360, 297-310.
- Noriega-Crespo A. (2002) *Rev. Mexicana Astron. Astrofis. Conf. Ser.*, 13, 71-78.
- O'Connell B., Smith M. D., Davis C. J., Hodapp K. W., Khanzadyan T., and Ray T. (2004) *Astron. Astrophys.*, 419, 975-990.
- O'Connell B., Smith M. D., Froebrich D., Davis C. J., and Eislöffel J. (2005) *Astron. Astrophys.*, 431, 223-234.
- Ostriker E. C. (1997) *Astrophys. J.*, 486, 291-306.
- Ostriker E. C., Lee C.-F., Stone J. M., and Mundy L. G. (2001) *Astrophys. J.*, 557, 443-450.
- O'Sullivan S. and Ray T. P. (2000) *Astron. Astrophys.*, 363, 355-372.
- Palau A., Ho P. T. P., Zhang Q., Estalella R., Hirano N., et al. (2006) *Astrophys. J.*, 636, L137-L140.
- Palumbo M. E., Geballe T. R., and Tielens A. G. G. M. (1997) *Astrophys. J.*, 479, 839-844.
- Pudritz R. E. and Banerjee R. (2005) In *IAU Symp. 227: "Massive Star Birth: A Crossroads of Astrophysics"* (R. Cesaroni et al., eds.), pp. 163-173. Cambridge Univ., Cambridge.
- Puga E., Feldt M., Alvarez C., and Henning T. (2005) *Poster presented at IAU Symp. 227: "Massive Star Birth: A Crossroads of Astrophysics"*.
- Quillen A. C., Thorndike S. L., Cunningham A., Frank A., Guter-

- muth R. A., et al. (2005) *Astrophys. J.*, 632, 941-955.
- Raga A. C. and Cabrit S. (1993) *Astron. Astrophys.*, 278, 267-278.
- Raga A. C., Cantó J., Calvet N., Rodríguez L. F., and Torrelles J. M. (1993) *Astron. Astrophys.*, 276, 539-548.
- Raga A. C., Cabrit S., and Cantó J. (1995) *Mon. Not. R. Astron. Soc.*, 273, 422-430.
- Raga A. C., Beck T., and Riera A. (2004a) *Astrophys. Space Sci.*, 293, 27-36.
- Raga A. C., Noriega-Crespo A., González R. F., and Velázquez P. F. (2004b) *Astrophys. J. Suppl.*, 154, 346-351.
- Raga A. C., Williams D. A., and Lim A. (2005) *Rev. Mexicana Astron. Astrofis.*, 41, 137-146.
- Rawlings J. M. C., Redman M. P., Keto E., and Williams D. A. (2004) *Mon. Not. R. Astron. Soc.*, 351, 1054-1062.
- Reipurth B., Bally J., and Devine D. (1997) *Astron. J.*, 114, 2708-2735.
- Richer R. S., Shepherd D. S., Cabrit S., Bachiller R., and Churchwell E. (2000) In *Protostars and Planets IV*, (V. Mannings et al., eds.), pp. 867-894. Univ. of Arizona, Tucson.
- Ridge N. A. and Moore T. J. T. (2001) *Astron. Astrophys.*, 378, 495-508.
- Rodríguez L. F., Carral P., Moran J. M., and Ho P. T. P. (1982) *Astrophys. J.*, 260, 635-646.
- Rodríguez L. F., Torrelles J. M., Anglada G., and Martí J. (2001) *Rev. Mexicana Astron. Astrofis.*, 37, 95-99.
- Rodríguez L. F., Garay G., Brooks K. J., and Mardones D. (2005a) *Astrophys. J.*, 626, 953-958.
- Rodríguez L. F., Poveda A., Lizano S., and Allen C. (2005b) *Astrophys. J.*, 627, L65-L68.
- Rosen A. and Smith M. D. (2004a) *Astron. Astrophys.*, 413, 593-607.
- Rosen A. and Smith M. D. (2004b) *Mon. Not. R. Astron. Soc.*, 347, 1097-1112.
- Sandell G. and Knee L. B. G. (2001) *Astrophys. J.*, 546, L49-L52.
- Schilke P., Walmsley C. M., Pineau des Forêts G., and Flower D. R. (1997) *Astron. Astrophys.*, 321, 293-304.
- Schreyer K., Semenov D., Henning T., and Forbrich J. (2006) *Astrophys. J.*, 637, L129-L132.
- Shepherd D. S. (2003) In *ASP Conf. Ser. 287: "Galactic Star Formation Across the Stellar Mass Spectrum"* (J. M. De Buizer and N. S. van der Blik, eds.), pp. 333-344. Astronomical Society of the Pacific, San Francisco.
- Shepherd D. S. (2005) Massive Molecular Outflows. In *IAU Symp. 227: "Massive Star Birth: A Crossroads of Astrophysics"* (R. Cesaroni et al., eds.), pp. 237-246. Cambridge Univ., Cambridge.
- Shepherd D. S. and Kurtz S. E. (1999) *Astrophys. J.*, 523, 690-700.
- Shepherd D. S., Watson A. M., Sargent A. I., and Churchwell E. (1998) *Astrophys. J.*, 507, 861-873.
- Shepherd D. S., Yu K. C., Bally J., and Testi L. (2000) *Astrophys. J.*, 535, 833-846.
- Shepherd D. S., Borders T., Claussen M., Shirley Y., and Kurtz S. (2004) *Astrophys. J.*, 614, 211-220.
- Shu F. H., Ruden S. P., Lada C. J., and Lizano S. (1991) *Astrophys. J.*, 370, L31-L34.
- Smith M. D. and Rosen A. (2003) *Mon. Not. R. Astron. Soc.*, 339, 133-147.
- Smith M. D. and Rosen A. (2005) *Mon. Not. R. Astron. Soc.*, 357, 579-589.
- Smith M. D., Suttner G., and Yorke H. W. (1997) *Astron. Astrophys.*, 323, 223-230.
- Sollins P. K., Hunter T. R., Battat J., Beuther H., Ho P. T. P., et al. (2004) *Astrophys. J.*, 616, L35-L38.
- Stanke T., McCaughrean M. J., and Zinnecker H. (2000) *Astron. Astrophys.*, 355, 639-650.
- Stahler S. W. (1994) *Astrophys. J.*, 422, 616-620.
- Stone J. M. and Hardee P. E. (2000) *Astrophys. J.*, 540, 192-210.
- Suttner G., Smith M. D., Yorke H. W., and Zinnecker H. (1997) *Astron. Astrophys.*, 318, 595-607.
- Tafalla M. and Myers P. C. (1997) *Astrophys. J.*, 491, 653-662.
- Tafalla M., Bachiller R., Wright M. C. H., and Welch W. J. (1997) *Astrophys. J.*, 474, 329-345.
- Tafalla M., Santiago J., Johnstone D., and Bachiller R. (2004) *Astron. Astrophys.*, 423, L21-L24.
- Tafaya D., Gómez Y., and Rodríguez L. F. (2004) *Astrophys. J.*, 610, 827-834.
- Takakuwa S., Ohashi N., and Hirano N. (2003) *Astrophys. J.*, 590, 932-943.
- Torrelles J. M., Patel N. A., Anglada G., Gómez J. F., Ho P. T. P., et al. (2003) *Astrophys. J.*, 598, L115-L119.
- van Dishoeck E. F. (2004) *Ann. Rev. Astron. Astrophys.*, 42, 119-167.
- van der Tak F. F. S. and Menten K. M. (2005) *Astron. Astrophys.*, 437, 947-956.
- van der Tak F. F. S., Boonman A. M. S., Braakman R., and van Dishoeck E. F. (2003) *Astron. Astrophys.*, 412, 133-145.
- Velusamy T. and Langer W. D. (1998) *Nature*, 392, 685-687.
- Viti S. and Williams D. A. (1999) *Mon. Not. R. Astron. Soc.*, 310, 517-526.
- Viti S., Codella C., Benedettini M., and Bachiller R. (2004) *Mon. Not. R. Astron. Soc.*, 350, 1029-1037.
- Völker R., Smith M. D., Suttner G., and Yorke H. W. (1999) *Astron. Astrophys.*, 343, 953-965.
- Wakelam V., Caselli P., Ceccarelli C., Herbst E., and Castets A. (2004) *Astron. Astrophys.*, 422, 159-169.
- Wakelam V., Ceccarelli C., Castets A., Lefloch B., Loinard L., et al. (2005) *Astron. Astrophys.*, 437, 149-158.
- Walker C. K., Carlstrom J. E., and Bieging J. H. (1993) *Astrophys. J.*, 402, 655-666.
- Watson C., Zweibel E. G., Heitsch F., and Churchwell E. (2004) *Astrophys. J.*, 608, 274-281.
- White G. J. and Fridlund C. V. M. (1992) *Astron. Astrophys.*, 266, 452-456.
- Wilkin F. P. (1996) *Astrophys. J.*, 459, L31-L34.
- Williams J. P., Plambeck R. L., and Heyer M. H. (2003) *Astrophys. J.*, 591, 1025-1033.
- Wiseman J., Wootten A., Zinnecker H., and McCaughrean M. (2001) *Astrophys. J.*, 550, L87-L90.
- Wu Y., Wei Y., Zhao M., Shi Y., Yu W., Qin S., and Huang M. (2004) *Astron. Astrophys.*, 426, 503-515.
- Yamashita T., Suzuki H., Kaifu N., Tamura M., Mountain C. M., and Moore T. J. T. (1989) *Astrophys. J.*, 347, 894-900.
- Yokogawa S., Kitamura Y., Momose M., and Kawabe R. (2003) *Astrophys. J.*, 595, 266-278.
- Yorke H. W. and Sonnhalter C. (2002) *Astrophys. J.*, 569, 846-862.
- Yu K. C., Billawala Y., and Bally J. (1999) *Astron. J.*, 118, 2940-2961.
- Yu K. C., Billawala Y., Smith M. D., Bally J., and Butner H. M. (2000) *Astron. J.*, 120, 1974-2006.
- Zhang Q. and Zheng X. (1997) *Astrophys. J.*, 474, 719-723.
- Zhang Q., Hunter T. R., Sridharan T. K., and Ho T. P. T. (2002) *Astrophys. J.*, 566, 982-992.
- Zhang Q., Hunter T. R., Brand J., Sridharan T. K., Cesaroni R., et al. (2005) *Astrophys. J.*, 625, 864-882.